

Ameliorative effect of carveol on scopolamine-induced memory impairment in rats

Komal Latif^{1*}, Saneela Saneela¹, Arif-ullah Khan¹

¹ Riphah Institute of Pharmaceutical Sciences, Riphah International University, Islamabad

ARTICLE INFO

Article type:

Original

Article history:

Received: Jul 17, 2022

Accepted: Oct 9, 2022

Keywords:

Alzheimer

Amnesia

Anti-inflammatory

Anti-oxidant

Carveol

Memory impairment

Neuroinflammation

ABSTRACT

Objective(s): Carveol is a naturally occurring terpenoid with antispasmodic, carminative, astringent, indigestion, and dyspepsia properties, as well as anti-diabetic, anti-oxidant, anti-hyperlipidemia, and anti-inflammatory properties in the liver. Research also suggests that it has memory-enhancing and anti-oxidant properties. The purpose of this research was to see whether carveol could protect rats against scopolamine-induced memory loss in a rat model.

Materials and Methods: Thirty male Sprague-Dawley rats (200–250 g) were grouped as the saline group receiving saline, disease group receiving scopolamine, and four treatment groups among which three groups received scopolamine+carveol and one group received scopolamine+donepezil for 28 days. Followed by *in vitro*, behavioral, anti-oxidant, and molecular studies were done. $P < 0.005$ was considered statistically significant.

Results: The *in vitro* assay showed that carveol caused diphenyl-1-picrylhydrazyl inhibition. *In-vivo* findings revealed that carveol (50, 100, and 200 mg/kg) significantly improved dementia by reducing escape latency and spending more time in the targeted quadrant in the Morris water maze test. Increased number of entries and percent spontaneous alterations were observed in rats' Y-maze test. In animal brain tissues, i.e., cortex and hippocampus, carveol enhanced glutathione, glutathione-S-transferase, catalase, and reduced lipid peroxide levels. Carveol also improved cellular architecture in histopathological examinations and decreased expression of inflammatory markers such as amyloid-beta, nuclear factor kappa light chain activated B cells, tumor necrosis factor-alpha, cyclooxygenase 2, prostaglandin E2, and interleukin-18, as evidenced by immunohistochemistry and enzyme-linked immunosorbent assays, as well as molecular investigations.

Conclusion: This study suggests that the compound could be potent against amnesia mediated through anti-oxidant, amyloid-beta inhibition, and anti-inflammatory pathways.

► Please cite this article as:

Latif K, Saneela S, Khan AU. Ameliorative effect of carveol on scopolamine-induced memory impairment in rats. Iran J Basic Med Sci 2022; 25: 1504-1512. doi: <https://dx.doi.org/10.22038/IJBMS.2022.66797.14647>

Introduction

Alzheimer's disease (AD), schizophrenia, epilepsy, and depression all have cognitive loss as common characteristics (1, 2). AD is a multifactorial neurodegenerative disease that often begins slowly and is progressively fatal (3, 4). Risk factors for the development of AD include hypertension, hyperlipidemia, heart disease, and diabetes (5). In 2015, a report estimated about 46.8 million people with dementia cases worldwide (6, 7). As the prevalence of its number is continually growing, it is expected to double every 20 years, 74.7 million people are expected to be affected by AD 2030 (8). Low-middle-income nations now account for 58 percent of the world's aging population with dementia, with the prevalence projected to rise to 68 percent by 2050 (9). There is a high prevalence, due to the percentage of elderly people increasing more quickly, in populous nations like China, Pakistan, and their South Asian and Western Pacific neighbors (10). Pakistan is the world's sixth most populous nation, with an estimated percentage of dementia cases of 150,000–200,000 people (11).

AD is characterized by a psychological and behavioral disturbance that ends in the loss of memory, impairment of cognition, plaques of amyloid-beta (A β) protein, and amyloid accumulation of 39-42 AA peptides (12).

Deposition of the amyloid precursor protein, neurofibrillary tangles, and abnormal tau protein filaments deposition in the form of intraneuronal neurofibrillary tangles generate free radicals which ultimately cause synaptic dysfunction, neurotoxicity, and neuroinflammation (13). An abnormal decrease in the levels of acetylcholine in the brain and phosphorylation of tau proteins deteriorates forebrain and cholinergic neurons disrupt the neuronal pathways and neurotransmitters involved in the process of learning and memory (14). In neurodegenerative illnesses such as Alzheimer's disease, Parkinson's disease, and ischemic brain damage, synaptic disruption and excessive generation of oxidative stress indicators reduce memory capacity (15, 16). In these neurodegenerative diseases, disturbances in metabolic pathways such as loss of ionic gradient, release of excitatory neurotransmitters, and production of harmful radicals all lead to death (17). Scopolamine, a muscarinic cholinergic receptor antagonist, is an effective pharmacological drug for creating a partial amnesia model (18). As a result, scopolamine may be useful in both animal models of amnesia and in defining prospective cognition-enhancing medicines (19).

Carveol is a naturally occurring terpenoid found in *Mentha spicata* and *Carum carvi* essential oils (20, 21). Carveol has been used for antispasmodic, carminative,

*Corresponding author: Komal Latif. Riphah Institute of Pharmaceutical Sciences, Riphah International University, Islamabad, Pakistan. Email: komallatifk@gmail.com

astringent, indigestion, and dyspepsia in traditional Chinese medicine (22). Its anti-diabetic, anti-oxidant, anti-hyperlipidemia, and anti-inflammatory properties in the liver are also shown (23). The current study aims to investigate the anti-amnesic potential of carveol, employed *in vitro*, *in vivo*, and in molecular techniques.

Materials and Methods

Chemicals

Carveol, donepezil, and scopolamine hydrobromide were purchased from Sigma (St. Louis, USA). Dimethyl sulfoxide (DMSO) was purchased from Merck Millipore (Billerica, MA, USA). Antibodies (anti-A, anti-NF- κ B, anti-TNF-, and anti-COX-2) from rats, 3, 3-diaminobenzidine peroxidase (DAB), Avidin-Biotin Complex (ABC), 1-chloro-2,4-dinitrobenzene (CDNB), hydrogen peroxide (H₂O₂), trichloroacetic acid (TCA), formalin, thiobarbituric acid (TBA) were purchased from St. Louis, MO, USA. The secondary antibody was obtained from Abcam in the United Kingdom. Rat A β , rat NF- κ B, rat TNF- α , rat IL-18, and rat PGE2 ELISA kits were obtained from Elabscience China.

Animals

In this experiment, male Sprague-Dawley rats weighing 200–250 g were utilized and kept in the animal house of Riphah Institute of Pharmaceutical Sciences (RIPS) in Islamabad (n=30, 5 in each group). Experiments were carried out with the approval of RIPS' Research and Ethics Committee (Ref. No. REC/RIPS/2020/14) and in accordance with the Principles of Laboratory Animal Care. A 12/12 hr light-dark cycle and relative humidity at 55% \pm 5% were maintained, and the room temperature was controlled at 25 $^{\circ}$ C \pm 1 $^{\circ}$ C. *Ad libitum* food and water were available.

Study design

Rats were divided into 6 groups.

Group 1: Saline group received 10 ml/kg normal saline containing 5% DMSO intraperitoneal (IP).

Group 2: Disease group received five injections of Scopolamine (1 mg/kg, IP) dissolved in a mixture of normal saline and 5% DMSO for 28 days.

Group 3: Treatment group received Scopolamine (1 mg/kg) daily, followed by carveol (50 mg/kg) IP for 28 days.

Group 4: Treatment group received scopolamine (1 mg/kg) daily, followed by carveol (100 mg/kg) IP for 28 days.

Group 5: Treatment group received scopolamine (1 mg/kg) daily, followed by carveol (200 mg/kg) IP for 28 days.

Group 6: Treatment group received scopolamine (1 mg/kg) daily, followed by donepezil (5 mg/kg) IP for 28 days.

Two hr after the scopolamine injection, carveol and donepezil were dissolved in mixture of normal saline and 5% DMSO and injected intraperitoneally. Rats were taught for the Morris water maze test on the 29th, 30th, and 31st days, and a probe test was performed on the 32nd day to evaluate spatial learning. On day 33, we conducted three trials of the Y-maze test for memory impairment and observed spontaneous behavior change. On the same day, all groups of rats were terminally anesthetized with sodium pentobarbital (60 mg/kg, IP) before being decapitated. Tissues were collected and centrifuged in phosphate-buffered saline (0.1 M PBS), pH 7.4, 5% w/v. Using a micropipette, the supernatant was collected and stored at -80 $^{\circ}$ C. (n=5/group) Brain tissues were extracted and subjected to anti-oxidant and molecular testing, and maintained in 4 percent formaldehyde for paraffin block production to process and analyze Hematoxylin and Eosin

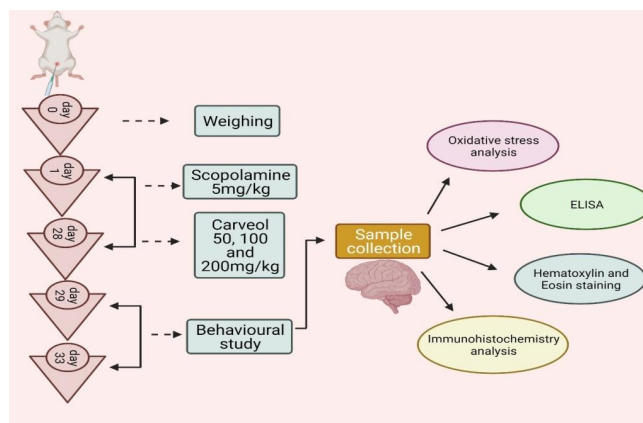


Figure 1. Schematic diagram of the experiment protocol

(H&E) and immunohistochemistry (IHC) examination. The experimental protocol is described in Figure 1.

DPPH free radical scavenging assay

The ability of the compounds to scavenge free radicals was tested using 1,1-diphenyl, 2-picrylhydrazyl (DPPH). Different dilutions (1.25, 2.50, 5, 10, 20 μ g/ml) of compounds (0.1 ml) were added to 0.004 % methanolic solution of DPPH. A UV spectrophotometer was used to measure the absorbance at 517 nm after 30 min. Ascorbic acid was utilized as positive control.

The scavenging activity was measured as a percentage:

$$\left(\frac{A_0 - A_1}{A_0} \right) \times 100$$

A1 is the absorbance of the chemical sample, while A0 is the absorbance of the control. Inhibition curves were generated using the GraphPad Prism software (GraphPad, San Diego, California, USA) to obtain the values of median inhibitory concentrations in each experiment. (IC₅₀) (24).

Morris water maze (MWM) test

The standard technique outlined by elements of learning and memory in rats is utilized in conjunction with the MWM test [14]. This experiment was carried out in a big circular tank (120 cm diameter x 50 cm height, with a colored round platform 1 cm below the water's surface) with the platform fixed for a visual cue. To estimate the escape latency time (time to locate hidden platform), rats were taught to identify the hidden platform with a maximum latency time of 180 seconds at the start of the experiment, and swim distance was recorded in each trail across three trail days for three consecutive days. During the probe test, each rat was dropped without a platform opposite to the targeted quadrant, and time spent in the targeted quadrant was measured by using a stopwatch (22, 25).

Y-maze test

The y-maze was conducted in a y-maze device that had three identical arms, each measuring 40 cm long, 35 cm high, and 12 cm broad. Rats were put in the arm's middle and permitted to freely roam throughout the labyrinth. To calculate spontaneous changes, five sessions were conducted. The Y-maze spontaneous alteration was characterized as overlapping triplet sets of consecutive entries into each of the three arms (26).

Determination of anti-oxidant profile

GSH and GST assay

Freshly extracted brain tissue samples were homogenized (0.1 M PBS, pH 7.4), mixed with phenyl methyl sulfonyl fluoride (PMSF), and centrifuged (4000 x g) for 10 min at 4 °C. The GSH levels were determined by collecting the supernatant with a micropipette and using the previously described technique with minor changes [16]. To dissolve 0.6 mM DTNB, 2 ml of the following mixture was combined with 0.2 ml of previously collected supernatant in 0.2M PBS. To make up the final volume and collect 3 ml of solution, 0.1 M PBS was utilized. After 10 min, the absorbance was measured at a wavelength of 412 nm. PBS and DTNB solutions were used to adjust the absorbance values for the negative and positive controls, respectively. The GSH levels were calculated and represented in mol/mg of proteins. The GST level was similarly determined using a well-established technique with just minor changes [17]. A test solution containing 5 mM GSH and 1 mM CDNB was made with freshly produced PBS (0.1 M). In duplicate, 60 L of supernatant was added to a glass vial containing 1.2 ml of test solution. To make the blank solution in triplicate, distilled water was added in the same quantity. The absorbance of these prepared solutions (210 l) was measured using an ELISA microplate reader (max = 340 nm, 5 min at 23 °C). Total protein concentration was measured using a BCA kit according to the manufacturer's instructions, and the resulting GST values were represented in mol/mg of protein.

Catalase assay

The activity of catalase was determined by mixing 3 ml H₂O₂ with 0.05 ml tissue supernatant. At 240 nm, the absorbance activity was measured against a blank containing just 3 ml of PBS. The absorbance is proportional to the amount of H₂O₂ present, which is reduced when catalase destroys H₂O₂. This is a measurement of H₂O₂ breakdown and is given as mol H₂O₂ decomposed per milligram of protein per minute (27).

LPO Assay

Another important oxidative stress marker is LPO, which uses a colorimetric method to detect TBARS (thiobarbituric acid reactive compounds) (28). Each rat's cortical and hippocampal tissues were homogenized separately in 10 ml of 20 mM Tris-HCl at 4 °C in a Polytron homogenizer while maintaining a pH of 7.4. The supernatant was recovered after centrifuging the homogenate at 1000 g for 10 min at 4 °C. A new ferric ammonium sulfate solution was made. The collected supernatant received 40 microliters of the aforementioned solution, which was then incubated at 37 °C for 30 min. Then, 400 mg of 2-thiobarbituric acid (TBA) was dissolved in 50 ml of water to make a 0.8 percent solution. TBA was added to the supernatant and ferric ammonium sulfate mixture in a total of 75 liters. A plate reader was used to detect absorbance at a wavelength of 532 nm.

Hematoxylin and Eosin (H&E) staining

After deparaffinizing tissue slides with xylene (100 percent), slides are rehydrated. Then slides were rinsed in PBS and immersed in hematoxylin for a minimum of 10 min. The slides were then dehydrated by treating them with successive ethanol dilutions of 70, 95, and 100 percent, followed by xylene fixation and application of coverslips (28). Microscopic pictures were examined using

an Olympus light microscope (Olympus, Japan) and ImageJ NIH software. Each group received 5 microscopic pictures to evaluate neuron shape, cellular infiltration, and vacuole development.

Immunohistochemistry (IHC) investigation

The slides were deparaffinized and rehydrated before being treated with proteinase K to extract antigen. The slides were then washed in 0.1 M PBS before being immersed in 3 percent H₂O₂ for ten minutes to suppress peroxidase activity. Again slides were washed in 0.1 M PBS and incubated in a humidified room for at least one hour with normal goat serum (5 percent NGS with 0.1 percent Triton X-100). After treating slides with primary antibodies such as anti-A β , anti-NF- κ B, anti-TNF- α , and anti-COX-2, they were incubated overnight at 4 °C (Dilution 1:100, Santa Cruz Biotechnology, USA). The following day, the slides were washed twice with 0.1 M PBS before being incubated in a humidified room for one and a half hours with biotinylated secondary antibodies (dilution factor 1:50). After another wash with 0.1 M PBS, the slides were incubated in a humidified room for one hour with ABC. Finally, slides were stained with DAB, washed with water, and dehydrated, followed by xylene fixation and placement of coverslips following application of the mounting medium. A light microscope was used to acquire three microscopic pictures for each slide (Olympus, Japan). ImageJ was used to evaluate A β and NF- κ B expression, and relative integrated density was computed (29).

Enzyme-linked immunosorbent assay

The A β , NF- κ B, TNF- α , IL-18, and PGE2 ELISAs were performed according to the manufacturer's instructions. Following homogenizing a sufficient amount of brain tissues (50 mg), the supernatant was recovered after centrifugation (at 4000 x g for 30 min). The total protein concentration in each group was determined using the BCA method. Using a 96-well plate, protein samples were treated with antibodies supplied in the kit, and absorbance values were measured using a microplate reader. Concentrations in picograms per liter (pg/ml) were then adjusted to total protein content in pg/mg total protein. All steps were repeated three times (30).

Statistical analysis

Image J was used to evaluate the morphological data (9). The data is given as a mean with a standard error of the mean (31). Graph pad prism 6 was used to apply two-way ANOVA with *post hoc* Tukey's test. $P < 0.005$ was deemed statistically significant.

Results

Effect of carveol on DPPH free radicals scavenging inhibition

In DPPH free radical scavenging assay, increase in carveol concentrations, i.e., 1.25, 2.5, 5, 10, and 20 μ g/ml showed increased DPPH inhibition of 52.35 ± 0.45 , 59.85 ± 0.56 , 67.68 ± 0.45 , 76.50 ± 0.14 , and 82.12 ± 0.26 , respectively. At the same concentrations, ascorbic acid showed DPPH inhibition of 63.72 ± 0.51 , 71.37 ± 0.69 , 76.25 ± 0.55 , 82.65 ± 0.70 , and $87.51 \pm 0.62\%$ as shown in Figure 2.

Effect of carveol on cognitive impairment

In the MWM test, the escape latency time for the carveol was measured in three trials per day for three consecutive days. In the saline (10 mg/kg) group, escape latency at days 1, 2 and 3 was 19.0 ± 0.5 , 18 ± 0.5 , and 18.5 ± 0.6 sec,

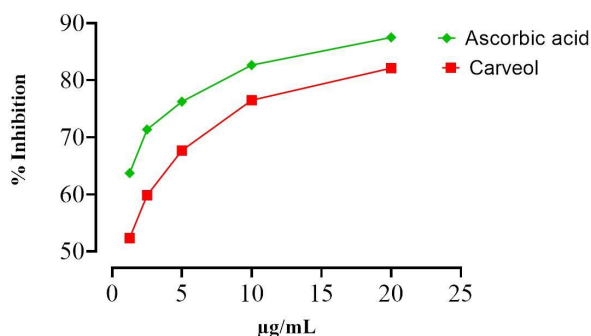


Figure 2. Anti-oxidant potential of carveol using the DPPH assay
DPPH: 1,1-diphenyl, 2-picrylhydrazyl

respectively. In the scopolamine (5 mg/kg) group, escape latency increased to 31.0 ± 0.3 , 35.0 ± 0.5 , 37.0 ± 0.3 sec, respectively. In the carveol (50 mg/kg) treated group, escape latency decreased to 29.0 ± 0.5 , 28.0 ± 0.5 , 23.0 ± 0.4 sec, respectively. In carveol (100 mg/kg) escape latency reduced to 27.0 ± 0.81 , 24.0 ± 0.14 , 20.0 ± 0.43 sec, respectively. In carveol (200 mg/kg) escape latency further reduced to 26.0 ± 0.5 , 21.0 ± 0.3 , 19.0 ± 0.9 sec, respectively. In donepezil (5 mg/kg) escape latency was 26.0 ± 0.4 , 19.0 ± 0.5 , 18 ± 0.3 sec, respectively vs scopolamine group as shown in Figure 3a. On the 4th day the duration spent in the desired quadrant by the scopolamine 5 mg/kg group was significantly lower, i.e., 21.0 ± 2 sec vs saline group 51.0 ± 1 sec, Figure 3b. The observed time spent in the target quadrant of carveol 50, 100, 200 mg/kg, and donepezil 5 mg/kg were significantly higher, i.e., 38 ± 1 , 41 ± 2 , 44 ± 1 , and 46 ± 1 sec vs the scopolamine group.

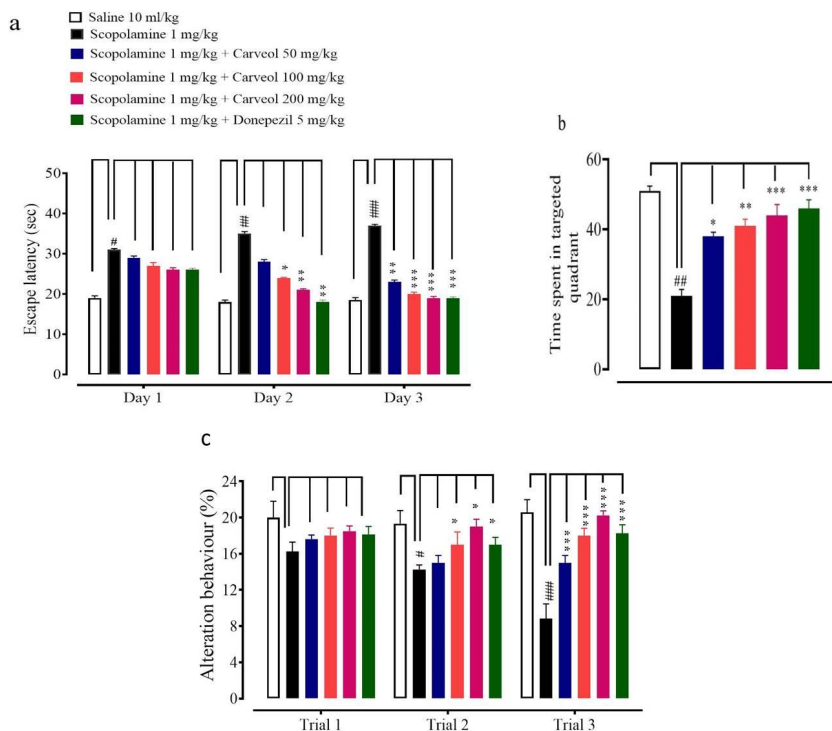
Effects on alteration behavior

The Y-maze task was performed to analyze the spatial

working memory using spontaneous alternation behavior (%). In the saline (10 mg/kg) group, spontaneous alterations at trials 1, 2, and 3 were 20 ± 1.80 , 19.32 ± 1.45 , 20.58 ± 1.40 , respectively. In scopolamine (5 mg/kg) group, spontaneous alterations reduced to 16.25 ± 1.04 , 14.27 ± 0.43 , 8.85 ± 1.39 , respectively. In carveol (50 mg/kg) treated group, spontaneous alterations increased to 17.62 ± 0.38 , 15 ± 0.71 , 15 ± 0.8 , respectively. In carveol (100 mg/kg) treated group, spontaneous alterations enhanced to 18.03 ± 0.71 , 17 ± 1.22 , 18 ± 0.71 , respectively. In carveol (200 mg/kg) treated group, spontaneous alterations further increased to 18.5 ± 0.5 , 19 ± 0.70 , 20 ± 0.43 , respectively. In donepezil (5 mg/kg) treated group, spontaneous alterations were 18.15 ± 0.75 , 17 ± 0.71 , 18.25 ± 0.82 (Figure 3c).

Effect on oxidative stress markers

In saline (10 ml/kg) group, GSH, GST, catalase, and LPO levels in cortex tissues were 9.56 ± 0.41 , $\mu\text{moles/mg}$, 7.10 ± 0.43 $\mu\text{moles CDNB conjugate/min/mg}$, 11.61 ± 0.45 $\mu\text{moles H}_2\text{O}_2/\text{min/mg}$, and 37.9 ± 2 nmoles/min/mg , respectively. In scopolamine (5 mg/kg) group GSH, GST, and catalase levels decreased to 6.57 ± 0.39 $\mu\text{moles/mg}$, 3.99 ± 0.07 $\mu\text{moles CDNB conjugate/min/mg}$, and 3.57 ± 0.51 $\mu\text{moles H}_2\text{O}_2/\text{min/mg}$, and LPO level increased to 122.78 ± 2.10 nmoles/min/mg , respectively. In carveol (200 mg/kg) treated group GSH, GST, catalase levels increased to 8.77 ± 0.19 $\mu\text{moles/mg}$, 6.37 ± 0.37 $\mu\text{moles CDNB conjugate/min/mg}$, and 9.23 ± 0.36 $\mu\text{moles H}_2\text{O}_2/\text{min/mg}$, and LPO level decreased to 83.57 ± 3 nmoles/min/mg , respectively. In donepezil (5 mg/kg) treated group GSH, GST, and catalase levels raised to 8.77 ± 0.19 $\mu\text{moles/mg}$, 6.46 ± 0.46 $\mu\text{moles CDNB conjugate/min/mg}$, and 9.0 ± 0.40 $\mu\text{moles H}_2\text{O}_2/\text{min/mg}$, and LPO level reduced to 77.48 ± 2.10 nmoles/min/mg , respectively (Figure 5). In saline (10 ml/kg) group GSH, GST, catalase, and LPO levels in hippocampus tissues were



Figures 3a, b, and c. Effects of carveol and donepezil on escape latency time of rats on days 1, 2, and 3 in Morris water maze test, time spent in the targeted quadrant and alteration behavior of rats on trials 1, 2, and 3 in the Y-maze test. Values expressed as mean \pm SEM (n=5). Two-way ANOVA with *post hoc* Tukey's test. # $P < 0.005$, ## $P < 0.001$, ### $P < 0.001$ vs saline group, * $P < 0.05$, ** $P < 0.01$, *** $P < 0.001$ vs scopolamine group

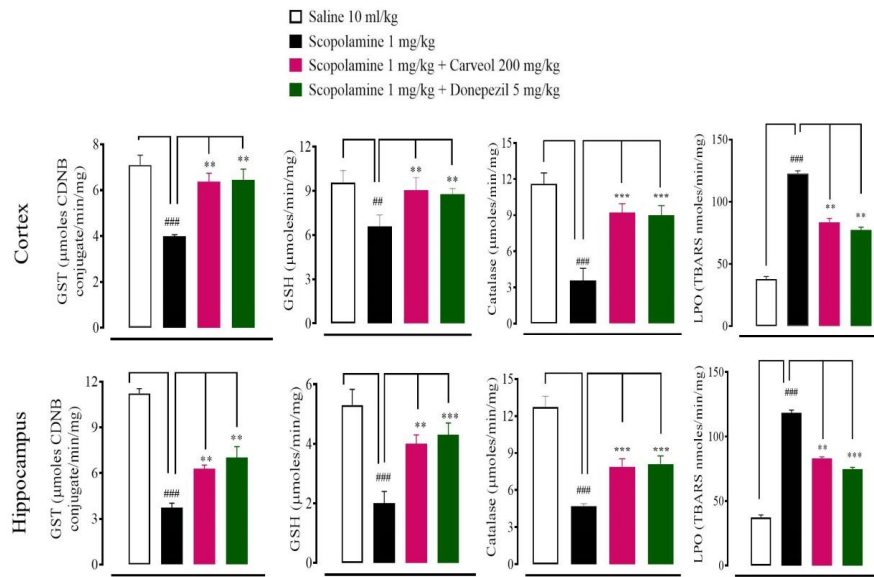


Figure 4. Effect of carveol and donepezil against reduced glutathione (GSH), glutathione-S-transferases (GST), catalase, and lipid peroxidation (LPO) in scopolamine-induced amnesic rat's cortex and hippocampus tissues. Data presented as mean ± SEM (n=5). Two-way ANOVA with *post hoc* Tukey's test. ##*P*<0.01, ###*P*<0.001 vs saline group, ***P*<0.01, ****P*<0.001 vs scopolamine group

5.3 ± 0.5 µmoles/mg, 11.23 ± 0.31 µmoles CDNB conjugate/min/mg, 12.72 ± 0.44 µmoles H₂O₂/min/mg, and 37.23 ± 2 nmoles/min/mg, respectively. In scopolamine (5 mg/Kg) group GSH, GST, and catalase levels decreased to 2 ± 0.4 µmoles/mg, 3.73 ± 0.30 µmoles CDNB conjugate/min/mg, and 4.71 ± 0.10 µmoles H₂O₂/min/mg, and LPO level was increased to 118.4 ± 2.10 nmoles/min/mg, respectively. In carveol (200 mg/kg) treated group GSH, GST, and catalase levels increased to 4 ± 0.3 µmoles/mg, 6.28 ± 0.25 µmoles CDNB conjugate/min/mg, and 7.90 ± 0.32 µmoles H₂O₂/min/mg, and LPO level decreased to 83.15 ± 1.05 nmoles/min/mg, respectively. In donepezil (5 mg/kg) treated group GSH, GST, and catalase level raised to 4.3 ± 0.4 µmoles/mg, 7.01 ± 0.73 µmoles CDNB conjugate/min/mg, and 8.11 ± 0.33 µmoles H₂O₂/min/mg, and LPO level reduced to 74.62 ± 1.50 nmoles/min/mg, respectively (Figure 4).

Histopathological examination

The saline (10 ml/kg) group revealed no distinct pathological changes in cortex and hippocampus tissues. The scopolamine (1 mg/Kg) group showed vigorous

histological changes in the cortex and hippocampus tissues of the rat's brain. Abnormal histological changes were shown in the scopolamine group which included altered morphology of neurons comprising abnormal changes in cell size, shape (i.e., swollen, irregular angled, vacuolated), and abnormal staining (i.e., cytoplasmic eosinophilia and nucleus basophilia) in the cortex and hippocampus tissues. Carveol (200 mg/kg) and donepezil (5 mg/kg) attenuated infarct and damaged cells (Figure 5).

Effect of carveol on neuroinflammation

To identify the significant involvement of inflammatory mediators in neuroinflammation induced by scopolamine, IHC was performed. Results revealed that the scopolamine (1 mg/kg) group revealed overexpression of Aβ, NF-κB, TNF-α, and COX-2 markers compared with the saline group in cortex and hippocampus tissues (Figure 5, ***P*<0.001 and ****P*<0.0001). Carveol (200 mg/kg) and donepezil (5 mg/kg) treated groups down-regulated the expressions of Aβ and NF-κB, TNF-α, and COX-2 in cortex and hippocampus tissues, relative to the scopolamine group (Figure 6). For

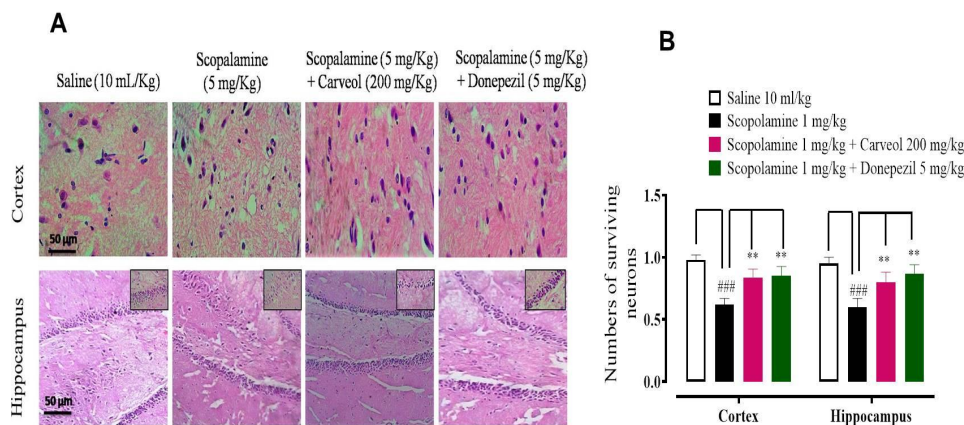


Figure 5. A and B represent the effect of carveol and donepezil against surviving neuron expression in rat's cortex and hippocampus tissues, using the hematoxylin and eosin histopathological staining technique. Bar 50 µm, magnification 40x. Values expressed as mean ± SEM (n=5). Two-way ANOVA with *post hoc* Tukey's test. ##*P*<0.001 vs saline group, ***P*<0.01, ****P*<0.001 vs scopolamine group

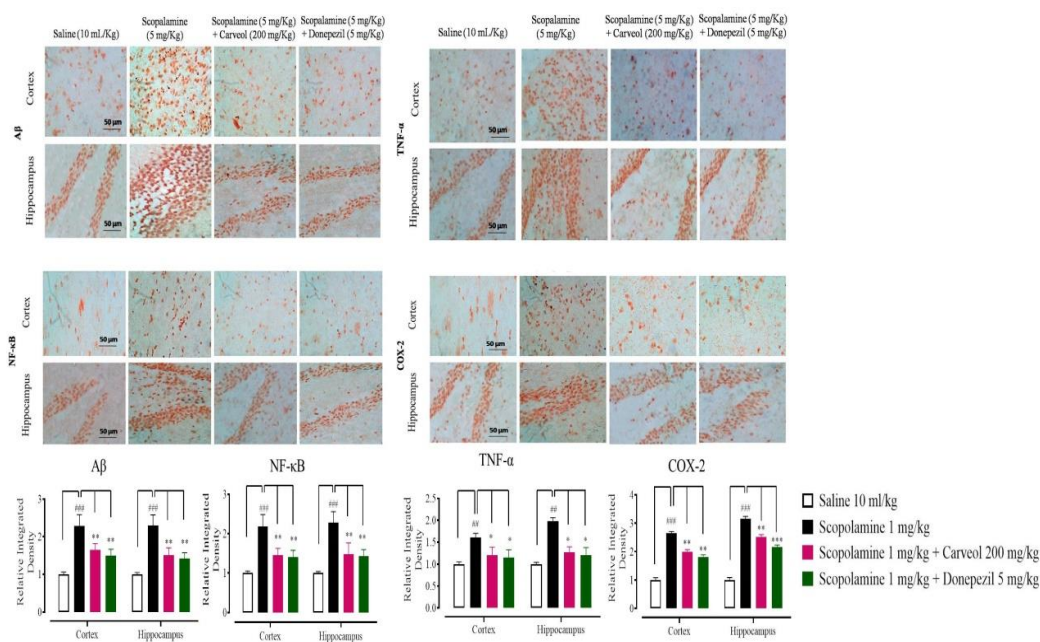


Figure 6. Inhibitory effects of carveol and donepezil against nuclear factor kappa Beta (NF-κB) expression in rats' cortex and hippocampus tissues, using the immunohistochemical technique. Bar 50 μm, magnification 40x. Values expressed as mean ± SEM (n=5). Two-way ANOVA with *post hoc* Tukey's test. ###*P*<0.001 vs saline group, ***P*<0.01, ****P*<0.001 vs scopolamine group

further validation, ELISA was performed and the results revealed that in the saline (10 ml/kg) group Aβ, NF-κB, TNF-α, IL-18, and PGE2 levels in cortex tissues were 720.33 ± 49.08, 1200 ± 40, 1400 ± 70, 295 ± 30, and 495 ± 30 pg/mg, respectively. In the scopolamine (5 mg/kg) group Aβ, NF-κB, TNF-α, IL-18, and PGE2 concentration increased to 2210 ± 119.3, 3030 ± 80, 2210 ± 80, 937 ± 35, and 837 ± 35 pg/mg, respectively. In the carveol (200 mg/kg) treated group Aβ, NF-κB, TNF-α, IL-18, and PGE2 production decreased to 1667.24 ± 49.90, 2030 ± 30, 1750 ± 100, 470 ± 40, and 700 ± 40 pg/mg, respectively. In the donepezil (5 mg/kg) treated group Aβ, NF-κB, TNF-α, IL-18, and PGE2 levels reduced to 1626.9 ± 95.37, 1580 ± 40, 1699 ± 70, 380 ±

30, and 680 ± 30 pg/mg, respectively. In the saline (10 ml/kg) group, Aβ, NF-κB, TNF-α, IL-18, and PGE2 concentration in hippocampus tissues were 587.17 ± 25.03, 1080 ± 30, 1350 ± 60, 274 ± 20, and 840 ± 50 pg/mg, respectively. In scopolamine (5 mg/kg) group Aβ, NF-κB, TNF-α, IL-18, and PGE2 production increased to 2537.1 ± 52.4, 3105 ± 90, 2105 ± 90, 840 ± 23, and 840 ± 50 pg/mg, respectively. In carveol (200 mg/kg) treated group Aβ, NF-κB, TNF-α, IL-18, and PGE2 concentration decreased to 1763.84 ± 98.78, 1880 ± 50, 1650 ± 110, 410 ± 30, and 680 ± 60 pg/mg, respectively. In donepezil (5 mg/kg) treated group Aβ, NF-κB, TNF-α, IL-18, and PGE2 production declined to 1480 ± 65.32, 1400 ± 50, 1610 ± 90, 310 ± 25, and 610 ± 60 pg/mg

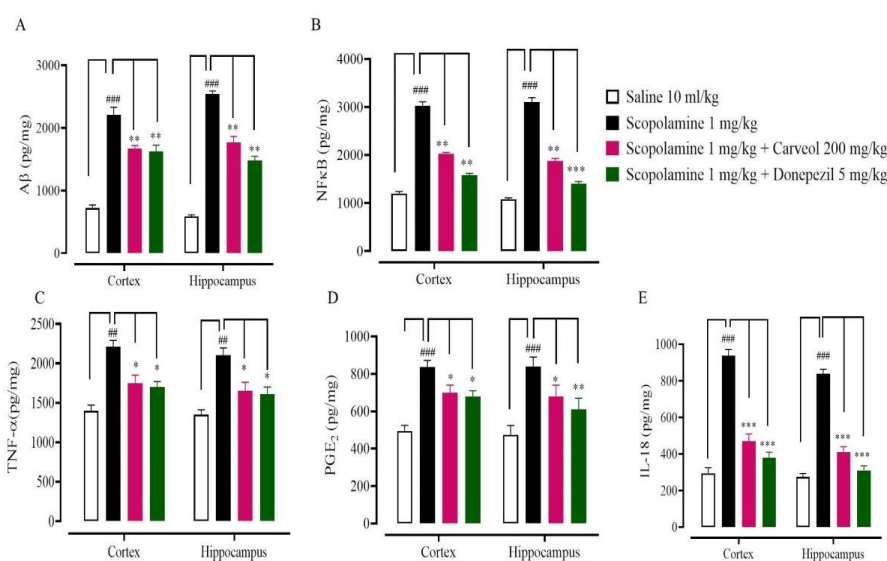


Figure 7. Inhibitory effect of carveol and donepezil against amyloid-beta (Aβ), nuclear factor kappa beta (NF-κB), tumor necrosis factor-alpha (TNF-α), interleukin-18 (IL-18), and prostaglandin E2 (PGE2) concentrations in rat's cortex and hippocampus tissues, using enzyme-linked immunosorbent assay technique. Values expressed as mean ± SEM (n=5). Two-way ANOVA with *post hoc* Tukey's test. ###*P*<0.001 vs saline group, ***P*<0.01, ****P*<0.001 vs scopolamine group

respectively (Figure 7).

Discussion

The impact of carveol on scopolamine-induced memory impairment in rats was studied *in vitro*, *in vivo*, and through biochemical and molecular tests. Scopolamine, a nonselective centrally acting muscarinic receptor antagonist, has long been recognized to impair learning and memory in rats and humans (19, 32). This memory impairment experimental paradigm has been widely utilized in research to find medicines with potential therapeutic benefits in dementia (33, 34).

Carveol's anti-oxidant capacity was first assessed *in vitro* using the DPPH free radical scavenging test, which revealed that it had greater anti-oxidant potential and was then investigated *in vivo*.

On behavioral tests, scopolamine reduced cognitive function. In order to test this effect, rats were given intraperitoneal injections of scopolamine to cause memory impairments. The MWM and Y-maze tests were used in behavioral research to look into their learning and memory abilities, while biochemical experiments were used to look into their potential molecular processes (35). In the current study, scopolamine-injected rats showed an increase in escape and latency when compared with the control groups. Similarly, as compared with the scopolamine-injected rats, the animals given carveol plus donepezil had a shorter escape latency. Carveol showed neuroprotective benefits against scopolamine-induced memory deficits, according to the results of behavioral experiments. The number of entries and spontaneous alternation behavior were used to measure spatial working memory, which is reliant on the hippocampus (36, 37). Increased cognitive performance is associated with a greater proportion of spontaneous modification behavior (38).

Carveol exhibited dose-dependent enhanced spontaneous alteration behavior and numerous entrances of rats in the Y-maze test in contrast to scopolamine-treated rats in the current research, indicating higher cognitive activities.

Scopolamine causes the deposition of A42 and A40, which are the end products of β -secretase amyloid precursor protein, which is produced by the cleaving of enzyme 1 (BACE1) (39). Increased BACE1 levels cause oxidative stress by activating JNK and p38 (40). Oxidative stress causes high oxygen consumption in the central nervous system, which contributes to AD pathogenesis (41, 42). According to previous research, oxidative stress is one of the first steps in the pathophysiology of memory loss (43). In the scopolamine group, oxidative damage was detected by low levels of GSH, GST, and catalase, and high levels of LPO, compared with carveol and donepezil, which had higher levels of GSH, GST, and catalase, and lower levels of LPO in the cortex and hippocampus. Our present findings indicate that scopolamine causes oxidative stress in the cortex and hippocampus of rats, as shown by reduced anti-oxidant enzyme activity, while carveol has neuroprotective effects via decreasing oxidative stress. Our results were in line with the findings of the other studies (44, 45): memory impairments caused by scopolamine are linked to the development of oxidative stress.

In addition, neuronal death was higher in the scopolamine group, while it was lower in the carveol group. Reduced neuronal loss in the cortex and the hippocampal

area was observed in the carveol-treated group, which was mediated via anti-oxidant and anti-inflammatory action. By signaling via toll-like receptors and advanced glycation end products, A β , which is generated by the cleavage of APP, forms aggregates that activate microglia. These receptors activate the NF- κ B transcription factors, which cause the generation of reactive oxygen species and the development of inflammatory mediators like cytokines (46, 47). TNF- α is a key pro-inflammatory cytokine in Alzheimer's disease (48). A β activates the transcription factor NF- κ B, which in turn increases TNF- α production in microglial cells (49). COX-2 is also strongly expressed in neurons, and its expression correlates with the presence of A deposits and tau tangles (50). Overexpression of COX-2 in neurons led to neuronal cell death in animal models of Alzheimer's disease by forming A plaques and producing free radicals, resulting in worsened cognitive impairments (51). IHC and ELISA were used to access A β , NF- κ B, TNF- α , COX-2, IL-18, and PGE2 levels in the rat brain and hippocampus in order to further verify the findings. All of these markers were increased in both areas in the scopolamine group, while carveol decreased the expression of these markers in the cortex and hippocampus, indicating its anti-inflammatory action. Carveol exhibited anti-amnesic potential by reducing A β synthesis and anti-inflammatory effects by substantially suppressing NF- κ B and TNF- α , resulting in reduced expression of pro-inflammatory cytokines, according to previous studies.

Conclusion

Scopolamine induced memory impairment and inflammation by activating various inflammatory mediators such as A β /NF- κ B/TNF- α /COX-2/IL-18, and PGE2 along with oxidative stress. Carveol exhibits an anti-amnesic effect, mediated through anti-oxidant, A β inhibition, and anti-inflammatory pathways, demonstrating its therapeutic potential in memory impairment.

Acknowledgment

We are thankful to Fareeha Anwar for partial technical support. The results presented in this paper were part of a student thesis. This research received no research grant from any funding organization.

Authors' Contributions

SS Conceptualized and designed experimental work, and conducted the experiment. KL Compiled the data and contributed to writing the manuscript, conducted *in vivo* anti-oxidant, ELISA, and immunohistochemistry assays. AK Supervised the whole study.

Conflicts of Interest

The authors declare no conflicts of interest.

References

- Haider S, Tabassum S, Perveen T. Scopolamine-induced greater alterations in neurochemical profile and increased oxidative stress demonstrated a better model of dementia: a comparative study. *Brain Res Bull* 2016; 127: 234-247.
- Kakeda S, Korogi Y. The efficacy of a voxel-based morphometry on the analysis of imaging in schizophrenia, temporal lobe epilepsy, and Alzheimer's disease/mild cognitive impairment: A review. *Neuroradiology* 2010; 52: 711-721.

3. Cavalli A, Bolognesi ML, Minarini A, Rosini M, Tumiatti V, Recanatini M, *et al.* Multi-target-directed ligands to combat neurodegenerative diseases. *J Med Chem* 2008; 51: 347-372.
4. Umar T, Hoda N. Alzheimer's disease: A systemic review of substantial therapeutic targets and the leading multi- functional molecules. *Curr Top Med Chem* 2017; 17: 3370-3389.
5. Selkoe DJ, Hardy J. The amyloid hypothesis of Alzheimer's disease at 25 years. *EMBO Mol Med* 2016; 8: 595-608.
6. McGill-Carter T. Market analysis Alzheimer's disease 2020. *J Psychiatry* 2020; 22: 21-22.
7. Wimo A, Guerchet M, Ali G-C, Wu Y-T, Prina AM, Winblad B, *et al.* The worldwide costs of dementia 2015 and comparisons with 2010. *Alzheimers Dement* 2017; 13: 1-7.
8. Guarino A, Favieri F, Boncompagni I, Agostini F, Cantone M, Casagrande M. Executive functions in Alzheimer disease: a systematic review. *Front Aging Neurosci* 2019; 10: 437.
9. Oliveira D, Jun Otuyama L, Mabunda D, Mandlate F, Gonçalves-Pereira M, Xavier M, *et al.* Reducing the number of people with dementia through primary prevention in Mozambique, Brazil, and Portugal: an analysis of population-based data. *J Alzheimers Dis* 2019; 70: S283-S291.
10. Burns A, Robert P. Dementia care: international perspectives. *Curr Opin Psychiatry* 2019; 32: 361-365
11. Thaver A, Ahmad A. Economic perspective of dementia care in Pakistan. *Neurology* 2018; 90: e993-e994.
12. FINDER VH, GLOCKSHUBER R. Amyloid- β aggregation. *Neurodegener Dis* 2007; 4: 13-27.
13. Carr D, Goate A, Phil D, Morris J. Current concepts in the pathogenesis of Alzheimer's disease. *Am J Med* 1997; 103: 3S-10S.
14. Deng Y, Xiong Z, Chen P, Wei J, Chen S, Yan Z. β -Amyloid impairs the regulation of N-methyl-D-aspartate receptors by glycogen synthase kinase 3. *Neurobiol Aging* 2014; 35: 449-459.
15. Belaidi AA, Bush AI. Iron neurochemistry in Alzheimer's disease and Parkinson's disease: targets for therapeutics. *J Neurochem* 2016; 139: 179-197.
16. Prolla TA, Mattson MP. Molecular mechanisms of brain aging and neurodegenerative disorders: lessons from dietary restriction. *Trends Neurosci* 2001; 24: 21-31.
17. Schemmert S, Schartmann E, Zafiu C, Kass B, Hartwig S, Lehr S, *et al.* A β oligomer elimination restores cognition in transgenic Alzheimer's mice with full-blown pathology. *Mol Neurobiol* 2019; 56: 2211-2223.
18. Hailwood JM, Heath CJ, Phillips BU, Robbins TW, Saksida LM, Bussey TJ. Blockade of muscarinic acetylcholine receptors facilitates motivated behaviour and rescues a model of antipsychotic-induced amotivation. *Neuropsychopharmacology* 2019; 44: 1068-1075.
19. Buccafusco JJ. The revival of scopolamine reversal for the assessment of cognition-enhancing drugs. 2nd ed. Boca Raton (FL): CRC Press/Taylor & Francis; 2011.
20. Guo J, Zhang R, Ouyang J, Zhang F, Qin F, Liu G, *et al.* Stereodivergent synthesis of carveol and dihydrocarveol through ketoreductases/ene-reductases catalyzed asymmetric reduction. *ChemCatChem* 2018; 10: 5496-5504.
21. De Carvalho CC, Da Fonseca MMR. Carvone: Why and how should one bother to produce this terpene. *Food Chem* 2006; 95: 413-422.
22. Agrahari P, Singh DK. A review on the pharmacological aspects of *Carum carvi*. *J Biol Earth Sci* 2014; 4: 1-13.
23. Ahmed MS, Khan A-u, Kury LTA, Shah FA. Computational and pharmacological evaluation of carveol for antidiabetic potential. *Front Pharmacol* 2020; 11: 919.
24. Adamson MM, Shakil S, Sultana T, Hasan MA, Mubarak F, Enam SA, *et al.* Brain injury and dementia in Pakistan: current perspectives. *Front Pharmacol* 2020; 11: 299-306.
25. Rahnema S, Rabiei Z, Alibabaei Z, Mokhtari S, Rafeian-Kopaei M, Deris F. Anti-amnesic activity of Citrus aurantium flowers extract against scopolamine-induced memory impairments in rats. *Neuro Sci* 2015;36: 553-560.
26. Hritcu L, Cioanca O, Hancianu M. Effects of lavender oil inhalation on improving scopolamine-induced spatial memory impairment in laboratory rats. *Phytomedicine* 2012; 19: 529-534.
27. Condon ME, Petrillo Jr EW, Ryono DE, Reid JA, Neubeck R, Puar M, *et al.* Angiotensin-converting enzyme inhibitors: importance of the amide carbonyl of mercaptoacyl amino acids for hydrogen bonding to the enzyme. *J Med Chem* 1982; 25: 250-258.
28. Latif K, Khan A-u, Izhar Ul Haque M, Naeem K. Bergapten attenuates nitroglycerin-induced migraine headaches through inhibition of oxidative stress and inflammatory mediators. *ACS Chem Neurosci* 2021;12: 3303-3313.
29. Shah FA, Zeb A, Ali T, Muhammad T, Faheem M, Alam SI, *et al.* Identification of proteins differentially expressed in the striatum by melatonin in a middle cerebral artery occlusion rat model—a proteomic and *in silico* approach. *Front Neurosci* 2018; 12: 888-902.
30. Malik I, Shah FA, Ali T, Tan Z, Alattar A, Ullah N, *et al.* Potent natural anti-oxidant carveol attenuates MCAO-stress induced oxidative, neurodegeneration by regulating the Nrf-2 pathway. *Front Neurosci* 2020; 14: 659-674.
31. Ala M, Ghasemi M, Mohammad Jafari R, Dehpour AR. Beyond its anti-migraine properties, sumatriptan is an anti-inflammatory agent: A systematic review. *Drug Dev Res* 2021; 82: 896-906.
32. Klinkenberg I, Blokland A. The validity of scopolamine as a pharmacological model for cognitive impairment: A review of animal behavioral studies. *Neurosci Biobehav Rev* 2010; 34: 1307-1350.
33. El-Sherbiny DA, Khalifa AE, Attia AS, Eldenshary EE- DS. Hypericum perforatum extract demonstrates anti-oxidant properties against elevated rat brain oxidative status induced by amnesic dose of scopolamine. *Pharmacol Biochem Behav* 2003; 76: 525-533.
34. Sharma D, Puri M, Tiwary AK, Singh N, Jaggi AS. Antiamnesic effect of stevioside in scopolamine-treated rats. *Indian J Pharmacol* 2010; 42: 164-167.
35. Oh JH, Choi BJ, Chang MS, Park SK. Nelumbo nucifera semen extract improves memory in rats with scopolamine-induced amnesia through the induction of choline acetyltransferase expression. *Neurosci Lett* 2009; 461: 41-44.
36. Holcomb L, Gordon MN, McGowan E, Yu X, Benkovic S, Jantzen P, *et al.* Accelerated Alzheimer-type phenotype in transgenic mice carrying both mutant amyloid precursor protein and presenilin 1 transgenes. *Nat Med* 1998; 4: 97-100.
37. Lelong V, Lhonnear L, Dauphin F, Boulouard M. BIMU 1 and RS 67333, two 5-HT 4 receptor agonists, modulate spontaneous alternation deficits induced by scopolamine in the mouse. *Naunyn-Schmiedeberg Arch Pharmacol* 2003; 367: 621-628.
38. Ali T, Badshah H, Kim TH, Kim MO. Melatonin attenuates D-galactose-induced memory impairment, neuroinflammation and neurodegeneration via RAGE/NF-KB/JNK signaling pathway in aging mouse model. *J Pineal Res* 2015; 58: 71-85.
39. Niikura T, Tajima H, Kita Y. Neuronal cell death in Alzheimer's disease and a neuroprotective factor, humanin. *Curr Neuropharmacol* 2006; 4: 139-147.
40. Mouton-Liger F, Paquet C, Dumurgier J, Bouras C, Pradier L, Gray F, *et al.* Oxidative stress increases BACE1 protein levels through activation of the PKR-eIF2 α pathway. *Biochim Biophys Acta* 2012; 1822: 885-896.
41. Li J, Li W, Jiang Z-G, Ghanbari HA. Oxidative stress and neurodegenerative disorders. *Int J Mol Sci* 2013; 14: 24438-24475.
42. Agostinho P, A Cunha R, Oliveira C. Neuroinflammation, oxidative stress and the pathogenesis of Alzheimer's disease. *Curr*

Pharm Des 2010; 16: 2766-2278.

43. Manral A, Meena P, Saini V, Siraj F, Shalini S, Tiwari M. DADS analogues ameliorated the cognitive impairments of Alzheimer-like rat model induced by scopolamine. *Neurotox Res* 2016; 30: 407-426.

44. Chen W, Cheng X, Chen J, Yi X, Nie D, Sun X, et al. Lycium barbarum polysaccharides prevent memory and neurogenesis impairments in scopolamine-treated rats. *PLoS One* 2014; 9: e88076.

45. Lee J-S, Kim H-G, Lee H-W, Han J-M, Lee S-K, Kim D-W, et al. Hippocampal memory enhancing activity of pine needle extract against scopolamine-induced amnesia in a mouse model. *Sci Rep* 2015; 5: 1-10.

46. González-Reyes RE, Nava-Mesa MO, Vargas-Sánchez K, Ariza-Salamanca D, Mora-Muñoz L. Involvement of astrocytes in Alzheimer's disease from a neuroinflammatory and oxidative stress perspective. *Front Mol Neurosci* 2017; 10: 427-446.

47. Rosales-Corral SA, Acuña-Castroviejo D, Coto-Montes A, Boga JA, Manchester LC, Fuentes-Broto L, et al. Alzheimer's disease: pathological mechanisms and the beneficial role of melatonin. *J Pineal Res* 2012; 52: 167-202.

48. Wang W-Y, Tan M-S, Yu J-T, Tan L. Role of pro-inflammatory cytokines released from microglia in Alzheimer's disease. *Ann Transl Med* 2015; 3: 136.

49. Shi S, Liang D, Chen Y, Xie Y, Wang Y, Wang L, et al. Gx-50 reduces β -amyloid-induced TNF- α , IL-1 β , NO, and PGE2 expression and inhibits NF- κ B signaling in a mouse model of Alzheimer's disease. *Eur J Immunol* 2016; 46: 665-676.

50. Li Q, Wu Y, Chen J, Xuan A, Wang X. Microglia and immunotherapy in Alzheimer's disease. *Acta Neurol Scand* 2022; 145: 273-278.

51. Yang S-H. Cellular and molecular mediators of neuroinflammation in Alzheimer disease. *Int Neurol J* 2019; 23: S54.